Theoretical Modelling of Langmuir Monolayers

F. Schmid, C. Stadler, H. Lange
Johannes Gutenberg Universität Mainz, D55099 Mainz, Germany

February 1, 2008

Abstract -

We study coarse grained, continuum models for Langmuir monolayers by self consistent field theory and by Monte Carlo simulations. Amphiphilic molecules are represented by stiff chains of monomers with one end grafted to a planar surface. In particular, we discuss the origin of successive fluid-fluid transitions, the possible origin of tilt order and the factors which determine the direction of tilt.

Paper presented at the *9th International Conference on Surface and Colloid Science*, Sofia, Bulgaria, 6-12 July 1997.

1 Introduction

In this contribution, we present theoretical model calculations for monolayers of amphiphiles spread at the air/water interface, *i.e.*, Langmuir monolayers. Such monolayers have two particularly remarkable properties: First, at intermediate temperatures there exist two distinct regions of fluid-fluid coexistence – a "gas-liquid" coexistence region and an additional region at higher surface coverage, where "liquid condensed" domains are present in a "liquid expanded" (LE) environment. The transition from the liquid expanded state to the liquid condensed state is not first order in a strict sense. Long range electrostatic interactions between the amphiphile head groups prevent macroscopic phase separation, and lead to the formation of a superstructure of ordered domains instead. However, these domains are of mesoscopic size (μm), and the transition can be considered first order on smaller length scales[1]. The second noteable feature of Langmuir monolayers is a complex polymorphism of phases on the condensed side of the phase diagram, which differ from each other in tilt order, positional order and orientational order of the backbones of the chains[2]. Three different types of phases, all of them liquid, can coexist with the liquid expanded phase: an untilted phase, and tilted phases with the chains tilted in the direction of nearest neighbors (NN), or next nearest neighbors (NNN).

We shall focus on two questions here: The origin of the first order transition to the liquid expanded phase, and the factors which determine the occurrence and the direction of collective tilt. To this end, we study simplified models of endgrafted stiff chains using mean field methods and Monte Carlo simulations. In the next two sections, we discuss mean field arguments with the aim to gain some insight into these problems. Then, we present some results of Monte

Carlo simulations.

2 Transition Liquid Expanded/Liquid Condensed

The amphiphiles are modeled as chains of seven rodlike segments (length l_0, diameter A_0) and one head segment, which is confined to a planar surface by a harmonic potential. Our chains are thus relatively short. Assuming that one segment corresponds to roughly two CH_2 units, they model in a very idealized way molecules of the size of, *e.g.*, tetradecanoic acid. The chains are made stiff with a bond angle potential $u\, k_B T \widehat{U}(1 - \cos\theta)$ for the angle θ between adjacent segments. We choose $\widehat{U}(x)$ such that it has a global minimum at $x = 0$ (straight chains) and a local minimum at $x = 1/2$ (chain defects): $\widehat{U}(x) = 25x + 34x^2 - 400x^3 + 480x^4$. We note however that qualitatively similar results are obtained with the simpler form $\widehat{U}(x) = x$. The adjustable parameter u determines the stiffness of the chains. Chain segments interact *via* repulsive hard core interactions and attractive long range interactions. These are treated with a density functional formalism, discussed in detail in ref. [3]. In a mean field treatment, we also need to account for the anisotropy of the chains explicitly. We do so on the level of the second virial coefficient by adding an orientation dependent term: $B_2^{anis.}(\Phi) = v\, \frac{5}{16\pi}(3\cos^2\Phi - 1)$, where Φ is the angle between two interacting segments. The parameter v thus describes the anisotropy per segment of a chain.

The problem is solved using self consistent field theory. In short, segment density distribution functions are calculated for single chains in an inhomogeneous external field, which is in turn determined self consistently from the density distribution functions. One obtains density profiles (Figure 1) and free

energies.

Figure 2 shows a resulting phase diagram in the plane of chain anisotropy versus molecular area. One finds coexistence of a liquid phase and a gas phase (not shown in the figure), and a region of phase coexistence between two untilted liquid phases, bounded by a critical point at low chain anisotropy and a triple point at high chain anisotropy. Almost the same diagram is obtained when varying the chain stiffness at fixed chain anisotropy Since both the effect of segment interactions and the chain stiffness go down with increasing temperature, the v or u axis can also be interpreted as temperature axis.

Hence the phase behavior turns out bo be mainly driven by the chain stiffness and the chain anisotropy. One can infer the origin of the phase transition: It is the result of a competition between the conformational entropy of the chains, which favors a disordered expanded state, and the tendency of the chains to pack parallel to each other, which favors the more compact condensed state. The expanded phase is thus dominated by chain "melting", and the condensed state by collective chain alignment [3, 4]. We note that our mean field treatment does not include the possibility of hexatic order. Therefore the coexistence region ends in a critical point. If the condensed phase has hexatic order, the coexistence region ends in a multicritical point, and one gets a line of continuous Kosterlitz-Thouless type transitions at higher temperatures.

3 Collective Tilt

Collective tilt can be induced for a number of reasons [3]. In most cases, the dominant mechanism is presumably a simple mismatch between the sizes of the head segment and the tail segments. When the heads are large, the

best way for the tails to maintain optimal packing is to tilt collectively in one direction. This effect can already be modelled by a simple system of rigid rods attached to a head group, which is confined to a planar surface (Figure 3). The interaction energy of two rods of length L at grafting distance $\vec{r}$, with tilt direction $\vec{e}$, is given by

$$E(\vec{r},\vec{e}) = V_h(r) + \frac{1}{\sigma^2}\int_0^L \int_0^L dl\, dl'\, V_{LJ}(d), \tag{1}$$

where $d = |\vec{r} + (l-l')\vec{e}|$ is the distance between two infinitesimal elements on the rod. V_{LJ} is a truncated Lennard Jones potential

$$V_{LJ}(d) = \epsilon((\frac{\sigma}{d})^{12} - 2(\frac{\sigma}{d})^6 + 0.031) \quad (d \le 2); \qquad V_{LJ}(d) = 0 \quad \text{otherwise} \tag{2}$$

and the head potential $V_h(d)$ is purely repulsive

$$V_h(r) = \epsilon((\frac{\sigma_h}{r})^{12} - 2(\frac{\sigma_h}{r})^6 + 1) \quad (d \le \sigma_h); \qquad V_h(r) = 0 \quad \text{otherwise} \tag{3}$$

with the head size σ_h. Figure 4 shows the state of lowest energy ("ground state") for such a system. As a function of head size or surface pressure, one finds a sequence of tilting transitions: No tilt (U) at small head size or high surface pressure, tilt towards next nearest neighbors (NNN) at intermediate head size or surface pressure, and tilt towards nearest neighbours (NN) at large head size and low surface pressure.

Hence not only the presence of tilt, but also the direction of tilt appears to be determined by the size of the head groups. The latter result might seem somewhat unexpected. It results from an interplay of surface tension and volume packing effects in the monolayer. An intuition can be gained from closer inspection of Figure 3. As the chains tilt, the head lattice gets distorted in the direction of tilt. In case of tilt towards next nearest neighbors

(b), the chain can thus optimize the distance to the four direct neighbors of type (ii); in case of tilt towards nearest neighbors (a), only the distance to the two neighbors (i) can be optimized. Hence the chain packing in the bulk is better for next nearest neighbor tilt. On the other hand, due to the tilt induced lattice distortion all direct neighbors are pushed apart in the case of tilt towards nearest neighbors, and only the neighbors of type (ii) in the case of tilt towards next nearest neighbors. Hence large heads are more comfortable in an environment of chains tilted towards nearest neighbors.

The argument can be translated into a simple approximate expression for the free energy [5]. According to this simplified (analytical) treatment, one expects a transition from the untilted state to a state with tilt towards next nearest neighbors as soon as the head size σ_h becomes larger than the effective chain diameter r_t ($r_t \approx 0.93\sigma$ in our case). The direction of tilt is expected to switch towards nearest neighbors at

$$\sigma_h - r_t = 3.93 r_t L/(2\kappa(\Sigma + \Pi) \tag{4}$$

where L is the chain length, κ is the volume compressibility of the chains, Σ is the surface tension and Π is the surface pressure (cf. Figure 4).

4 Monte Carlo simulations

We have performed Monte Carlo simulations of systems of stiff bead-spring chains, with one head bead confined to a planar surface [6]. Tail beads which are not direct neighbors in the chain interact *via* the Lennard-Jones potential (2), and head beads interact with the repulsive potential (3). The beads are connected by bonds of length b, subject to the pseudoharmonic potential $V_{bl}(b) = -2\ln(1 - 25(b - b_0)^2)$, where the optimum bond length is

chosen $b_0 = 0.7\sigma$. The chains are made stiff with a bond angle potential $U(\theta) = 10(1 - \cos\theta)$. In our simulations, chains contain one head bead and six tail beads. System sizes are typically 144 chains. Figure 5 shows a configuration snapshot in the disordered phase.

A full account of our simulations with detailed discussions of the results will be published elsewhere ([7], see also [8]). Here, we just show the resulting phase diagram for heads of size $\sigma_h = 1.2\sigma$ (Figure 6). We find a number different condensed phases, tilted and untilted, and a transition to a disordered phase which is first order for temperatures below $T \approx 3\epsilon/k_B$. At small surface pressure, the tilted phase is tilted towards next nearest neighbors. As the pressure is increased, an additional phase with tilt towards nearest neighbors emerges. Hence our simulations basically confirm the physical picture, which we have obtained by mean field arguments.

5 Discussion

To summarize, we have shown that the theoretical study of simplified models for monolayers of amphiphiles helps to clarify some of the physics of phase transitions in these systems. In particular, we have demonstrated that the first order transition between the liquid expanded phase and the liquid condensed phase is essentially driven by the chains. The condensed phase is characterized by chain alignment, *i.e.*, efficient chain packing, whereas the expanded phase is dominated by chain disorder. Furthermore, we have studied the phenomenon of collective tilt and established a relationship between the size of the head groups, the surface pressure, and the direction of the tilt.

Our results are consistent with a number of experimental observations. For

example, it has been shown that the liquid expanded phase disappears when the carbon chains are perfluorinated, *i.e.*, made much stiffer. It can be brought back into existence by the introduction of flexible hydrocarbon spacers[9]. Thus chain flexibility turns out to be important in the liquid expanded phase.

Our claim, that the phase behavior is mainly driven by the chains, is furthermore supported by the "temperature effect"[10], according to which the addition of two CH_2 units to the chain has an effect similar to reducing the temperature by 10-20^{0}C. We have not calculated explicitly the influence of the chain length on the phase behavior. However, one can argue, within our model, that increasing the chain length roughly corresponds to making the chains more flexible and lowering the temperature simultaneously (see Ref. [3] for details).

Finally, we have provided a simple explanation for the sequence of tilt transitions as a function of surface pressure in fatty acid monolayers [2]. The relation between head size and tilt direction also accounts for the fact that tilt towards nearest neighbors can be suppressed by increasing the pH of the subphase [11], or by replacing the COOH head groups in part by smaller alcohol head groups [12, 13]

6 Acknowledgments

We have benefited from discussions with M. Schick, K. Binder, F.M. Haas and K. Binder. C.S. is supported by the Graduiertenkolleg on supramolecular systems in Mainz.

References

[1] H. Möhwald, Ann. Rev. Phys. Chem. **41**, 441 (1990).

[2] M. Knobler, R.C. Desai, Ann. Rev. Phys. Chem. **43**, 207 (1992).

[3] F. Schmid, Phys. Rev. E **55**, 5774 (1997).

[4] F. Schmid, M. Schick, J. Chem. Phys. **102**, 2080 (1995).

[5] F. Schmid, H. Lange, J. Chem. Phys. **106**, 3757 (1997).

[6] F.M. Haas, R. Hilfer, K. Binder, *J. Chem. Phys.* **102**, 2960 (1995); F.M. Haas, R. Hilfer, K. Binder, *J. Phys. Chem.*, **100**, 15290 (1996); F.M. Haas, R. Hilfer, *J. Chem. Phys.* **105**, 3859 (1996).

[7] C. Stadler *et al*, in preparation.

[8] F. Schmid, C. Stadler, H. Lange, Computer Simulations in Condensed Matter Physics X, Springer, Heidelberg 1997.

[9] S.W. Barton, A. Goudot, O. Bouloussa, F. Rondelez, B. Lin, F. Novak, A. Acero, S.A. Rice, J. Chem. Phys. **96**, 1343 (1992).

[10] A.M. Bibo, I.R. Peterson, Adv. Mat. **2**, 309 (1990).

[11] M.C. Shih, T.M. Bohanon, J.M. Mikrut, P. Zschack, P. Dutta, J. Chem. Phys. **96**, 1556 (1992).

[12] B. Fischer, E. Teer, C.M. Knobler, J. Chem. Phys. **103**, 2365 (1995).

[13] E. Teer, C.M. Knobler, C. Lautz, S. Wurlitzer, J. Kildae, T.M. Fischer, J. Chem. Phys. **106**, 1913 (1997).

Figure Captions

Figure 1: Density profiles obtained from self consistent field calculations in the direction z perpendicular to the interface for different molecular areas A. Long and short dashed lines show the center of mass densities of tail and head segments, respectively. The solid line shows a coarse grained density profile, which accounts for the finite extension of the segments. Units are: z, the segment length l_0; A, the segment diameter A_0; and densities, $1/(l_0 A_0)$. Parameters are $u = 2$ and $v = 13.7$.

Figure 2: Phase diagram obtained from self consistent field calculation in the plane of anisotropy per segment v and molecular area A (in units of the segment diameter A_0) at chain stiffness $u = 2$ (after Ref. [3]).

Figure 3: Side view of the rigid rod model (top) and top view of the head lattice (bottom). (i) and (ii) mark different types of direct neighbors.

Figure 4: Zero temperature phase diagram of the rigid rod model in the plane of head size σ_h (in units of σ) vs. surface pressure Π (in units of $\epsilon/k_B\sigma^2$) at rod length $L = 5\sigma$. Dashed lines indicate the prediction of eqn. (4) with $\Sigma = 6.7\epsilon/k_B\sigma^2$ (after Ref. [5]).

Figure 5: Configuration snapshot in the disordered phase. Parameters are: Pressure $\Pi = 40\epsilon/k_B\sigma^2$, temperature $T = 4\epsilon/k_B$ and head size $\sigma_h = 1.1\sigma$. (from Ref. [8]).

Figure 6: Phase diagram obtained from Monte Carlo simulations in the plane of pressure Π (in units of $\epsilon/k_B\sigma^2$) vs. temperature T (in units of ϵ/k_B) for head size $\sigma_h = 1.2\sigma$. The transition to the disordered phase is first order up to $T \approx 3\epsilon/k_B$ and possibly becomes second order at higher temperatures.

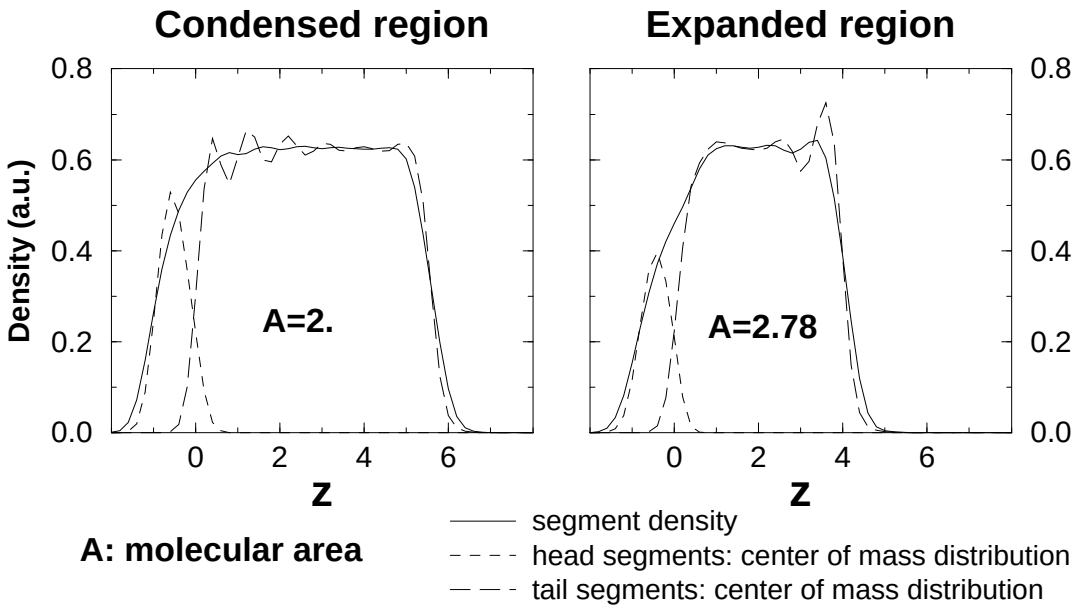

Figure 1
F. Schmid, C. Stadler, H. Lange

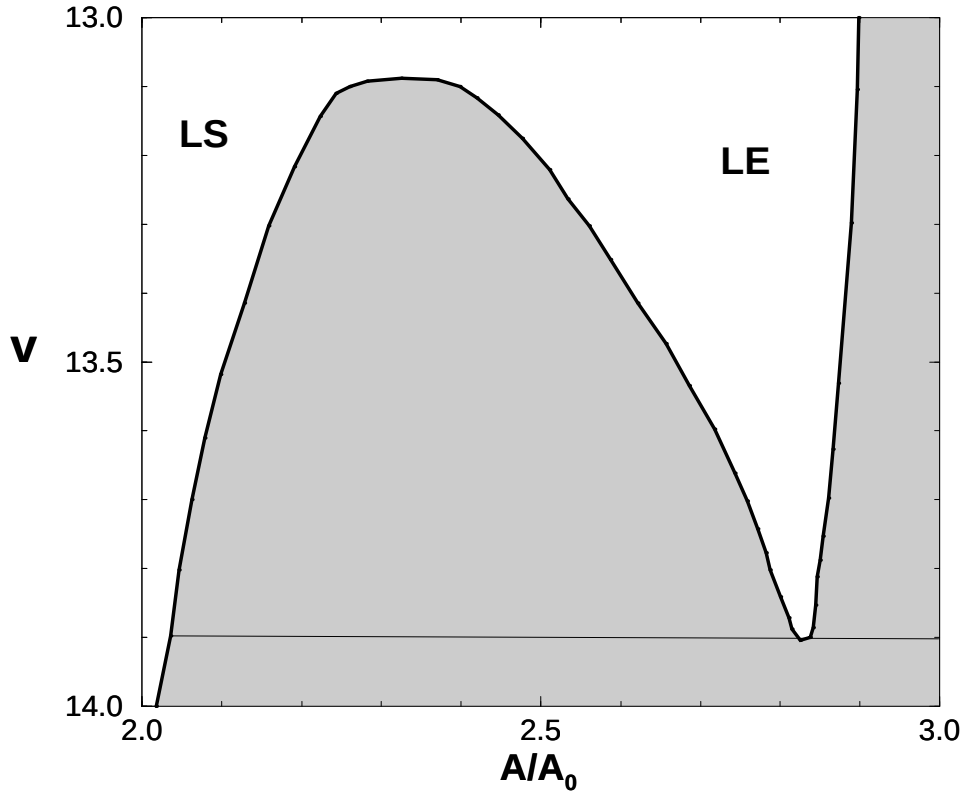

Figure 2
F. Schmid, C. Stadler, H. Lange

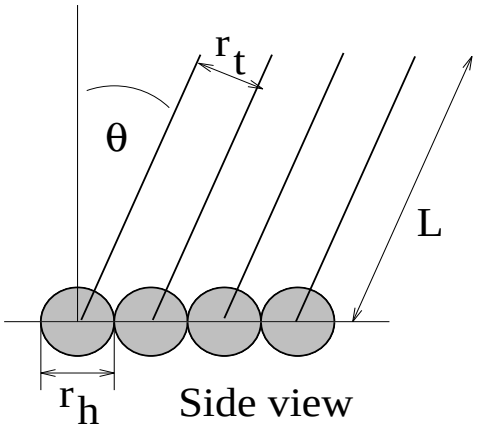

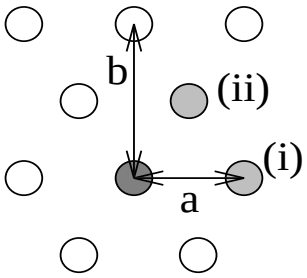

Head group lattice

Figure 3
F. Schmid, C. Stadler, H. Lange

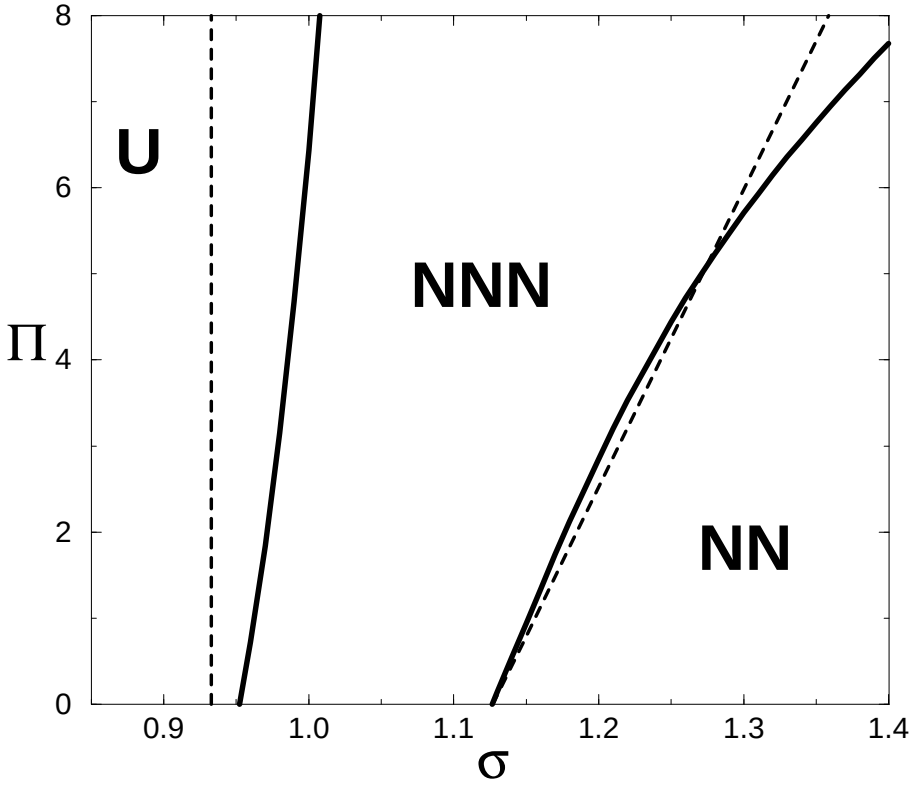

Figure 4
F. Schmid, C. Stadler, H. Lange

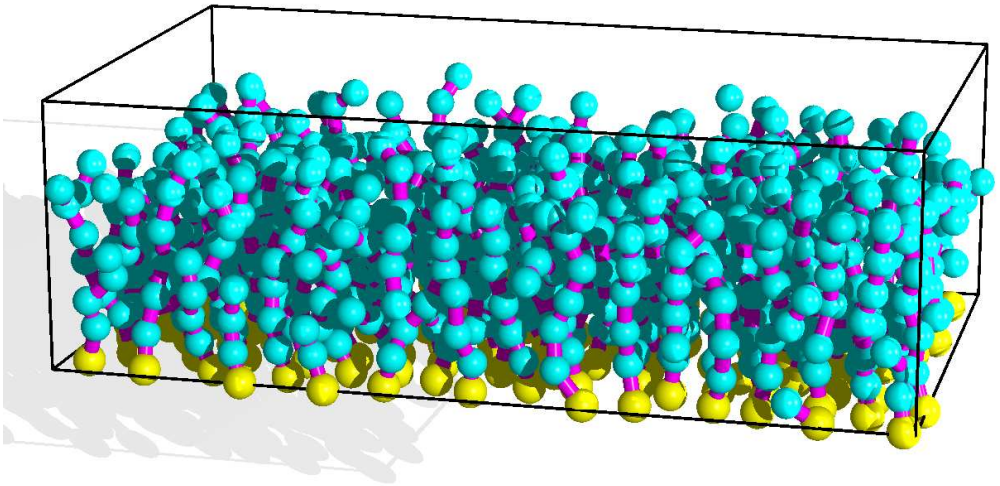

Figure 5
F. Schmid, C. Stadler, H. Lange

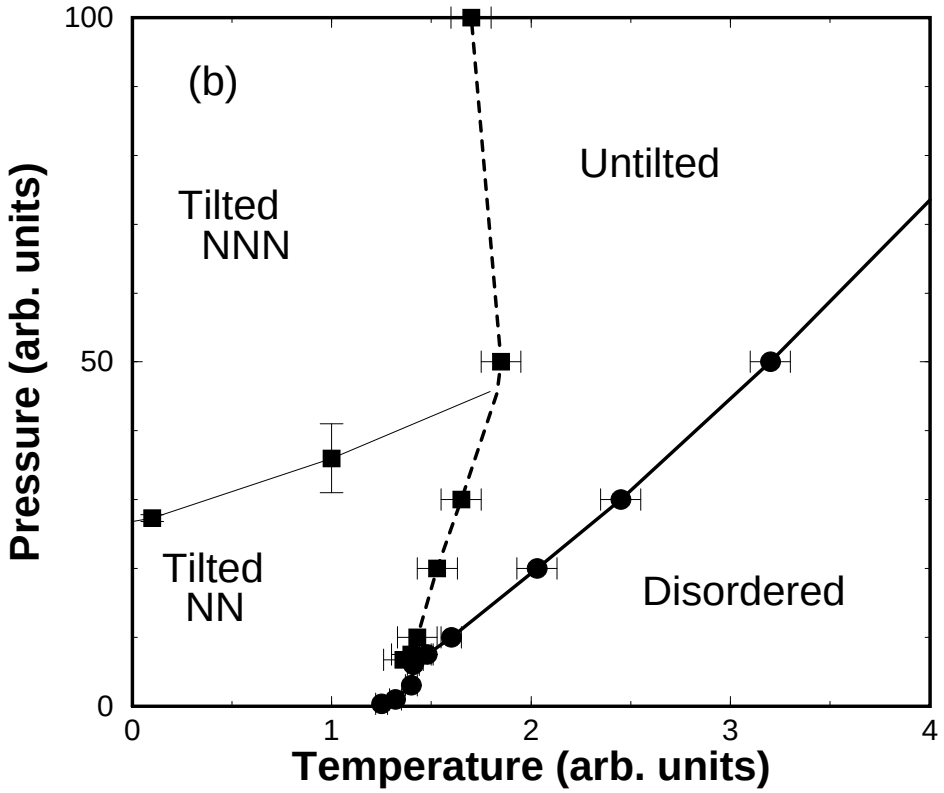

Figure 6
F. Schmid, C. Stadler, H. Lange